

Rodmanochytrium* is a new genus of chitinophilic chytrids (*Chytridiales*)*Martha J. Powell, Peter M. Letcher, William J. Davis, Rebecca B. Holland**

Department of Biological Sciences, The University of Alabama, Tuscaloosa AL 35487, USA

and

Carlos G. Vélez

Universidad de Buenos Aires, Facultad de Ciencias Exactas y Naturales. Depto., Biodiversidad y Biología Experimental & CONICET- Universidad de Buenos Aires, Instituto de Micología y Botánica (INMIBO), Buenos Aires, (C1428EHA) Argentina

ABSTRACT

From biodiversity surveys of aquatic habitats using chitin and pollen baits with samples collected in Argentina and the United States, we found a clade of eight chytrid strains with morphologies distinct from other described chytrids. After bringing these strains into axenic culture, we studied their thallus development and molecular phylogeny. Thalli produce operculate sporangia of variable shapes, ranging from spherical, pyriform to multilobed, and with rhizoidal systems exhibiting a sub-sporangial tube or swelling. Surfaces of sporangia could be smooth or ornamented. Resting spores are endobiotic when strains are grown on sweet gum pollen. Molecular phylogeny of 28S rDNA sequences place these eight strains in the *Chytriomycetaceae*. Based on thallus morphology, molecular phylogeny and zoospore ultrastructural features, we classify these eight strains as a new genus, *Rodmanochytrium*, containing two species, *R. sphaericum* and *R. pyriforme*. Published on-line www.phytologia.org *Phytologia* 101(3): 175-187 (Sept 21, 2019). ISSN 030319430.

KEY WORDS: *Rodmanochytrium* M.J. Powell & Letcher, *gen. nov.*, *Rodmanochytrium sphaericum* M.J. Powell & Letcher, *sp. nov.*, *Rodmanochytrium pyriforme* M.J. Powell & Letcher, *sp. nov.*, chitin, chytrid, *Chytridiomycota*, morphology, phylogeny, pollen, systematics

Recent explorations of aquatic habitats for chytrids have revealed that there is much undescribed diversity within the *Chytridiales* (Lefèvre et al., 2012; Leshem et al., 2016; Letcher and Powell, 2018; Letcher et al., 2014a, 2014b, 2018; Picard et al., 2009; Powell et al., 2013, 2018, 2019; Seto and Degawa, 2018; Seto et al., 2017; Vélez et al., 2013). From surveys of pollen and chitin-inhabiting chytrids, we isolated eight unidentified strains. Several of these unidentified isolates have been included in earlier molecular phylogenetic studies but never described. In a broad survey of *Chytridiomycetes*, strain WB 235A placed in the *Chytridiales* (James et al., 2006). In broad surveys of *Chytridiales*, several of the strains placed sister of the type species of *Chytriomycetes*, *C. hyalinus*, in the *Chytriomycetaceae* (strains ARG 12, ARG 39, WB 235A; Davis et al., 2015; Letcher and Powell, 2014; Letcher et al., 2014a, 2018; Powell et al., 2018). Letcher and Powell (2014) determined that zoospore ultrastructure of strains WB235A, ARG12, and ARG39 was a Group 1-type as Barr (1980) first characterized. These results support classification in *Chytriomycetaceae* based on the following zoospore ultrastructural character states: i. nucleus partially inserted into ribosomal aggregation; ii. kinetosome-associated structure (KAS) consists of stacked plates; iii. microtubular root includes multiple microtubules in a bundle; iv. microbody-lipid globule (MLC) complex cisterna fenestrated; v. flagellar plug bi-concave and thin (~90nm); and vi. paracrystalline inclusion large (vol. > 0.03 μm^3) (Letcher and Powell, 2014). Because of the distinct morphology and phylogenetic placement of these chytrid strains, we characterize a new genus, *Rodmanochytrium*, comprised of two species.

MATERIALS AND METHODS

Locations where strains used in this study were collected are listed in Table 1. Pine pollen, sweet gum pollen, dragonfly wings, and purified shrimp exoskeleton chitin strips were added as baits to aquatic samples. Strains were isolated and cultured on PmTG agar as described (Powell et al., 2019). Strains growing on natural substrates or nutrient media were observed with bright field and Nomarski interference contrast optics (Powell et al., 2019). Strains growing on chitin were prepared for scanning electron microscopy (SEM) and observed following the protocol in Picard et al. (2009).

DNA was extracted, purified and the partial large subunit rDNA gene (28S rDNA) amplified and sequenced as described previously (Powell et al., 2019). Eight new gene sequences, which we produced (noted in Table 1 with *), along with sequences downloaded from GenBank (Table 1), were aligned with Clustal X and manually adjusted in BioEdit (Powell et al., 2019). Phylogenetic analyses included 35 strains of in-group taxa rooted with strain JEL 222 *Rhizophyctium globosum* as the outgroup. Because of earlier phylogenetic placements, our analysis included 26 representatives of the morpho-species *Chytrium hyalinus*. *Rhopalophlyctis sarcoptoides* is included because of its sister position to *C. hyalinus*. Maximum parsimony (MP) trees were generated, maximum likelihood (ML) phylogenies constructed, and bootstrap support values calculated as described (Powell et al., 2019; Vélez et al., 2011). Sequence similarities among strains were determined with pairwise alignment in BioEdit (Hall, 1999).

RESULTS

For MP analysis, the dataset had 805 characters, of which 131 were parsimony informative. Of the 1005 trees derived from PAUPRat, all were equal in length ($L = 228$ steps) and were used to construct a single, strict consensus tree. For ML analysis, Modeltest selected HKY as the most appropriate model of nucleotide substitutions. The topologies of cladograms from MP and ML ($-\ln L = 956.58$) analyses were identical, with similar or equal support values. Minimum value for bootstrap support was set at 70%. Figure 1 shows the strict consensus tree from MP analysis, with ML/MP support values at nodes. Two major lineages (lineages A and B) were resolved.

Lineage A with $\geq 99\%$ bootstrap support included the eight unidentified strains in two sub-clades (A1, A2). Each of the sub-clades in lineage A is well supported, A1 with $\geq 98\%$ bootstrap support and A2 with 100% support. Interestingly in lineage A2, the two strains from Argentina show stronger relationships with strains from Alabama than they do with each other (Fig. 1). Within sub-clade A1, 28S rDNA sequence similarity is 98.0%; within subclade A2, sequence similarities range from 97.9–100%. Sub-clades A1 and A2 are divergent from each other, with strain MP 72 (sub-clade A1) having 93% sequence similarity with strain MP 41 (sub-clade A2). Thus, we consider that each of the two sub-clades in lineage A represents a species.

Lineage A is sister of lineage B ($\geq 79\%$ bootstrap support), which includes representatives of two other chitinophilic species (each the type species for their genus), *Rhopalophlyctis sarcoptoides* and the morpho-species *Chytrium hyalinus* (Fig. 1). The eight unidentified strains in lineage A are phylogenetically distinct from these other chitinophilic species in lineage B. For example, MP 72 in sub-clade A1 has only 88% sequence similarity with JEL 794 *Rhopalophlyctis sarcoptoides*. Thus, we consider members of lineage A as a distinct genus from *Rhopalophlyctis* and *Chytrium*.

TAXONOMY

Rodmanochytrium M.J. Powell & Letcher, *gen. nov.*

Mycobank no.: 830008

Typification: *Rodmanochytrium pyriforme* M.J. Powell & Letcher, sp. nov. (TYPE SPECIES).

Etymology: Named in honor of Dr. James E. Rodman, former program director in the Division of Environmental Biology at the US National Science Foundation, recognizing his implementation of the Partnerships for Enhancing Expertise in Taxonomy (PEET) program. This program targeted support for poorly studied groups of organisms, including chytrids, resulting in new species discovery, updated monographs, electronic access to data and a new generation of systematists trained.

Description: Sporangium: monocentric, epibiotic; pyriform, clavate, oval, or spherical, rarely lobed; surface smooth, hirsute, reticulate, rugose or finely granular; Rhizoid: rhizoidal axis emerges as a single tube from the sporangium, slightly swollen near the sporangium, dividing into branches near the sporangium; at maturity sub-sporangial portion tubular or swollen, rhizoidal system finely branched and pointed at the tips; dome-shaped septum separates rhizoids and sporangium. Zoospore Discharge: single, apical to lateral, relatively small operculate discharge pore; gelatinous plug forms below the operculum prior to discharge; operculum detached or hinged to side of pore after discharge; vesicular discharge with zoospores formed in sporangium, released as a quiescent mass, swarming and then swimming away. Zoospore: posteriorly uniflagellate, elongate, typically with a single lipid globule. Resting spore: typically endobiotic, globose or ovoid; thick walled with numerous lipid globules; germination not observed. Group 1-type zoospore. Monophyletic in *Chytriomycetaceae*.

Rodmanochytrium pyriforme M.J. Powell & Letcher, *sp. nov.*

Mycobank no.: 830009

Figs. 2, 3

Typification: UNITED STATES, Alabama, Washington County, Wagarville, Sullivan Lane, 31.4730583333, -88.037250. From a water and moist soil sample collected from a crawfish pond spring 2010 by J. K. Atchison and baited with chitin; strain MP 72 isolated by M. J. Powell, HOLOTYPE Fig. 2G, this publication.

Ex-Type Strain: MP 72 deposited in CZEUM (University of Michigan).

Etymology: The specific epithet refers to the predominant pyriform shape of the sporangium.

Description: Sporangium: predominantly pyriform, occasionally clavate, oval or spherical, rarely lobed; width at widest part typically 25-40 μm , sometimes up to 65 μm ; surface smooth, or rugose, often hirsute over the upper, expanded portion of the sporangium. Rhizoids: emergent from base of encysted zoospore as a slightly swollen tube; branches form near the sporangium and branch dichotomously; at maturity finely branched with pointed tips; dome-shaped septum separating rhizoids and sporangium. Zoospore Discharge: from a single, apical, sub-apical or lateral operculate discharge pore, which is relatively small; gelatinous plug forms beneath the operculum prior to zoospore discharge; operculum remains hinged to side of discharge pore or detaches; edge of discharge pore recurved; zoospores cleaved within sporangium, released as a motionless mass, after a quiescent period they begin to swarm and then swim away. Zoospore: elongate 4.5-5 μm long, typically with a single lipid globule. Resting spores: typically endobiotic; spherical or oval, 10-20 μm wide; containing numerous lipid globules; germination not observed. Saprotrophic on pollen and chitinous substrates.

Additional specimens examined: UNITED STATES, Alabama, Tuscaloosa County, Coker, Lake Lurleen. From an aquatic sample containing submerged vegetative matter, collected 29 February 2005 by W. H. Blackwell at the water's edge under an alder tree and baited with dragonfly wings; strain WB 235A isolated by M. J. Powell.

GenBank sequences of ex-type strain MP 72: MK543214 (28S rDNA).

Comments: Zoospores encyst and produce a long germ tube (Fig. 2A). The zoospore cyst enlarges into the incipient sporangium, which is typically pyriform (Figs. 2C, 3A); a small swelling forms on the rhizoidal axis at the base of the sporangium, and the rhizoidal axis branches (Figs. 2B, C, 2F). The enlarging sporangium is typically pyriform (see Kirk et al., 2008 for description of shapes), broad at the top and tapering toward the base (Figs. 2F-I, 3A, B, F-H). Occasionally the sporangium is oval, with a small cup-shaped base (Fig. 2D), or clavate (Fig. 2E). Sporangia are rarely irregular or lobed (Fig. 3D). Sporangial surfaces can be smooth (Fig. 3E), rugose (Fig. 3C, D) or hirsute, with hair-like structures covering the upper, expanded portion of the sporangium (Fig. 3E-I). The sub-sporangial rhizoid on mature sporangia may be branched with a slightly elongate (Figs. 2G, 3B) or spherical (Figs. 2L, 3C)

swelling joined to the tapered based of the sporangium through a short tube (Fig. 3F). A dome-shaped septum separates the sporangium from the rhizoidal system (Fig. 2L). Prior to zoospore discharge a gelatinous plug forms below the operculum (Fig. 2H). Zoospore discharge is vesicular (Fig. 2I), and the single, operculate discharge pore is apical (Fig. 2H, J), sub-apical (Figs. 2K) or lateral (Fig. 2I). The operculum remains attached to the side of the discharge pore (Fig. 2J) or becomes detached (Fig. 2K). The edge of the discharge pore is typically recurved (Fig. 2K). Spherical (Fig. 2M) or oval (Fig. 2N) resting spores are endobiotic in pollen. A tube connects the zoospore cyst at the surface of the pollen grain with the resting spore inside the pollen grain (Fig. 2M). Rather than enlarging into a sporangium, these zoospore cysts expel their contents into the pollen grain through the connecting tube in the process of resting spore formation (Fig. 2M).

Rodmanochytrium sphaericum M.J. Powell & Letcher, *sp. nov.*

Mycobank no.: 830010

Figs. 4, 5

Typification: UNITED STATES, Alabama, Tuscaloosa. From an aquatic sample containing *Myriophyllum* roots collected 5 June 2009 from a stream adjacent to 3621 Greensboro, Ave. and baited with chitin; strain MP 41 isolated by M. J. Powell, HOLOTYPE Fig. 4E, this publication.

Ex-Type Strain: MP 41 deposited in CZEUM (University of Michigan).

Etymology: The specific epithet refers to the predominant spherical shape of the sporangium.

Description: Sporangium: predominantly spherical, occasionally oval or pyriform, rarely lobed; width typically 20-55 μm , sometimes 70-110 μm ; surface smooth, reticulate, or finely granular. Rhizoids: emerge from the encysted zoospore as a single long germ tube with a slight swelling near the incipient sporangium; rhizoids branch near the sporangium and become bushy; at maturity rhizoids near sporangium are stout with dichotomous branches tapering to a pointed tip. Zoospore Discharge: from a single, operculate discharge pore, which is relatively small and typically apical; gelatinous plug forms beneath the operculum prior to zoospore discharge; operculum remains hinged to side of discharge pore or detaches; edge of discharge pore not recurved; zoospores cleaved within sporangium, released as a motionless mass, after a quiescent period zoospores begin to swarm and then swim away. Zoospore: elongate 4.5-5 μm long, typically with a single lipid globule. Resting Spores: not observed. Saprotrophic on pollen and chitinous substrates.

Additional specimens examined: UNITED STATES, Alabama, Wheeler National Wildlife Refuge. From an aquatic sample collected 9 August 2009 by B. Swan and baited with pollen; strains MP 59, MP 60, MP 61 isolated by M. J. Powell. ARGENTINA, Buenos Aires Province, Partido de Escobar, Paraná River floodplain. From an aquatic sample collected January 2005 from a rain pool and baited with pollen; strain ARG 12 isolated by C. G. Vélez. ARGENTINA, Corrientes Province. From an aquatic sample collected June 2006 from Chañar Stream and baited with pollen; strain ARG 39 isolated by C. G. Vélez.

GenBank sequences of ex-type strain MP 41: JX905522 (28S rDNA).

Comments: Zoospores encyst and produce an elongate germ tube (Fig. 4A). The portion of the germ tube near the encysted zoospore is slightly enlarged (Fig. 4B) and then branches, commonly dichotomously (Fig. 4C), or elongates into a trunk-like rhizoidal axis (Fig. 4D). Sporangia are typically spherical (Figs. 4E, G, H, J, K, 5A-D), but are sometimes oval (Fig. 4I) or broadly pyriform (Fig. 4F). The sporangial surface is variable, smooth (Fig. 5E), finely granular (Fig. 5A, B), or reticulate (Fig. 5B, C, D). The cytoplasm appears zoned in maturing sporangia; the central region is brown and granular and the periphery is yellowish and homogeneous (Fig. 4I). The branches of the primary rhizoidal axis often extend laterally on nutrient media (Fig. 4E), pollen (Fig. 4G) and chitin (Fig. 5A). On pollen the thallus can be epibiotic or interbiotic (Fig. 4G). Branches extending from the primary rhizoidal axis are stout near the sporangium (Fig. 4E, G-I), but continue dividing into fine branches with pointed tips (Fig. 4H, I). Zoospore discharge is vesicular (Fig. 4J), typically through an apical operculate discharge pore (Figs. 4J, K, 5D, E). The operculum remains hinged to the side of the discharge pore after zoospore release (Figs. 4K, 5E) or detaches.

DISCUSSION

Our results confirm earlier molecular phylogenetic studies of several of these unidentified strains (strains ARG 12, ARG 39, WB 235A) suggesting that they were members of the *Chytriomycetaceae* in the *Chytridiales* (Davis et al., 2015; Letcher and Powell, 2014; Letcher et al., 2014a, 2018). Previous ultrastructural analysis of zoospores of these isolates demonstrated characteristics consistent with other members of the *Chytriomycetaceae*, especially of the *Chytriomyces hyalinus* clade (Letcher and Powell, 2014).

Although thallus morphology in both of the two species of *Rodmanochytrium* is variable, typical of morphological plasticity found in other chytrids (Powell and Koch, 1977), the two species can be distinguished morphologically. Both species are rarely lobed, but this feature has been found as a variable characteristic in other related species, such as in *Chytriomyces hyalinus* shown to have crowding-induced irregularly-shaped sporangia (Roane and Paterson, 1974). The predominantly spherical shape of sporangia distinguishes *R. sphaericum* from *R. pyriforme* with predominantly pyriform sporangia, although *R. sphaericum* sporangia can sometimes be oval and rarely pyriform. The rhizoidal axes near the sporangium are stouter in *R. sphaericum* thalli than in *R. pyriforme* thalli. The main rhizoidal axis of *R. sphaericum* is typically a single short tube with a greater abundance of branches near the sporangium than in *R. pyriforme*. Also, *R. sphaericum* can produce sporangia in a larger size range than found with *R. pyriforme*. The edges of discharge pores on sporangia of *R. sphaericum* are even while those of *R. pyriforme* are recurved. Sporangial surfaces of both species may be smooth at thallus maturity, but some sporangia of *R. sphaericum* have reticulate surfaces while some sporangia of *R. pyriforme* have hirsute surfaces.

Chytrids producing sporangia with pyriform shapes are common, but *Rodmanochytrium* is distinct from these other described species. Unlike *Rodmanochytrium*, which is operculate, many of these are among the inoperculate chytrids, including *Podochytrium chitinophilum* (Willoughby, 1961), *Rhizophydium clavatum*, *R. clinopus*, *R. collapsum*, *R. obpyriformis*, *R. piriformis*, *R. utriculare* and *Phlyctochytrium indicum* (Karling, 1977; Sparrow, 1960). The operculate chytrids with pyriform sporangial shapes, such as *Chytridium cejpaii*, *C. lagenula*, *C. lecythii*, *C. pyriforme*, *C. rhizophyidi*, *C. sexuale*, *C. surirellae*, *C. versatile*, are parasitic (Karling, 1977; Sparrow, 1960), while *Rodmanochytrium* is saprotrophic.

In our phylogeny, *Rodmanochytrium* is sister of a clade including *Chytriomyces hyalinus* and *Rhopalophlyctis sacroptoides*, both operculate chytrids with vesicular zoospore discharge and the ability to grow on chitin-containing substrates. *Rodmanochytrium* is distinct from these other two genera. The endobiotic resting spore of *Rodmanochytrium* distinguishes it from *Chytriomyces*, which has epibiotic resting spores (Karling, 1945), although this can be a variable character (Roane and Paterson, 1974). In addition, *Rodmanochytrium* is not parasitic, as are members of *Chytriomyces* with pyriform shaped sporangia, including *Chytriomyces laevis*, *C. verrococus* and *C. willoughbyi* (Karling, 1960, 1968, 1987). The phylogenetic placement of *Rodmanochytrium* further demonstrates that it is not a member of the genus *Chytriomyces* because *C. hyalinus* is the type species of this genus (Letcher and Powell, 2002). The pyriform shaped sporangium in *Rodmanochytrium* is reminiscent of the *Rhopalophlyctis* thallus (Karling, 1945) but lacks the basal sterile cell found in the latter (Karling, 1945). Molecular sequence divergence of 28S rDNA between *Rodmanochytrium* and *Rhopalophlyctis* supports distinct genera (88% sequence similarity between strains MP 72 versus JEL 794).

Because chytrid thalli are relatively simple, morphological characters are often convergent because of limited ways to respond morphologically to natural selection. Similarly, morphological plasticity makes identification of chytrids based on thallus morphology alone difficult (Powell and Koch, 1977). This study demonstrates again that, in addition to thallus morphology, consideration of zoospore ultrastructural

characters and molecular phylogenetic placement is necessary to adequately characterize new taxa of chytrids (Letcher and Powell, 2014).

ACKNOWLEDGMENTS

This study was supported by the National Science Foundation through MRI DEB-0500766 (The University of Alabama) and REVSYS DEB-00949305 (M.P.). C.G.V. was supported by OAT 40/09 FCEN, University of Buenos Aires. We appreciate Will H. Blackwell (Professor Emeritus of Botany, Miami University), J. Keith Atchison, and Ben Swan for assistance in collection of samples for culture and S. Pennycook of Manaaki Whenua Landcare Research, Auckland, New Zealand, for assistance with nomenclatural issues. Sonali Roychoudhury (Patent Agent and Scientific Consultant, New York) and Kathryn Picard (Postdoctoral Fellow, Department of Botany, National Museum of Natural History, Smithsonian Institution, Washington, D. C.) provided insightful reviews of this manuscript.

LITERATURE CITED

- Barr, D. J. S. 1980. An outline for the reclassification of the *Chytridiales*, and for a new order, the Spizellomycetales. *Canad. J. Bot.* 58: 2380-2394.
- Davis, W. J., P. M. Letcher, J. E. Longcore and M. J. Powell. 2015. *Fayochytriomyces*, a new genus in *Chytridiales* (*Chytridiomycota*). *Mycologia* 107: 432-439.
- Hall, T. A. 1999. BioEdit: A user-friendly biological sequence alignment editor and analysis program for windows 95/98/NT. *Nucleic Acids Symp. Ser. (Oxf.)* 41: 95-98.
- James, T. Y., P. M. Letcher, J. E. Longcore, S. E. Mozley-Standridge, D. Porter, M. J. Powell, G. W. Griffith and R. Vilgalys. 2006. A molecular phylogeny of the flagellated fungi (*Chytridiomycota*) and description of a new phylum (*Blastocladiomycota*). *Mycologia* 98: 860-871, doi:10.3852/mycologia.98.6.860
- Karling, J. S. 1945. Brazilian chytrids. VI. *Rhopalophlyctis* and *Chytriomyces*. Two new chitinophyllic operculate genera. *Amer. J. Bot.* 32: 362-369.
- Karling, J. S. 1960. Parasitism among the chytrids. II. *Chytriomyces verrucosus* sp. nov. and *Phlyctochytrium synchytrii*. *Bull. Torrey Bot. Club.* 87: 326-336.
- Karling, J. S. 1968. Zoosporic fungi of Oceania. IV. Additional monocentric chytrids. *Mycopath. Mycol. Appl.* 36: 165-178.
- Karling, J. S. 1977. *Chytridiomycetorum Iconographia*. Lubrecht & Cramer, Monticello, NY.
- Karling, J. S. 1987. *Chytriomyces laevis* sp. nov., a virulent parasite of *Pythium*. *Nova Hedwigia* 44: 137-139.
- Kirk, P. M., P. F. Cannon, D. W. Minter and J. A. Stalpers. 2008. *Dictionary of the Fungi*, 10th edition, CAB International, Wallingford, United Kingdom.
- Lefèvre, E., P. M. Letcher and M. J. Powell. 2012. Temporal variation of the small eukaryotic community in two freshwater lakes: emphasis on zoosporic fungi. *Aquat. Microb. Ecol.* 67: 91-105.
- Leshem, T., P. M. Letcher, M. J. Powell and A. Sukenik. 2016. Characterization of a new chytrid species parasitic on the dinoflagellate, *Peridinium gatunense*. *Mycologia* 108: 731-743.
- Letcher, P. M. and M. J. Powell. 2002. A taxonomic summary of *Chytriomyces* (*Chytridiomycota*). *Mycotaxon.* 84: 447-487.
- Letcher, P. M. and M. J. Powell. 2014. Hypothesized evolutionary trends in zoospore ultrastructural characters in *Chytridiales* (*Chytridiomycota*). *Mycologia* 106: 379-396, doi:10.3852/13-219
- Letcher, P. M. and M. J. Powell. 2018. Morphology, zoospore ultrastructure, and phylogenetic position of *Polyphlyctis willoughbyi*, a new species in *Chytridiales* (*Chytridiomycota*). *Fungal Biol.* 122: 1171-1183.
- Letcher, P. M., J. E. Longcore and M. J. Powell. 2014a. *Dendrochytridium crassum*, a new genus in *Chytridiales* with unique zoospore ultrastructure. *Mycologia* 106: 145-153.

- Letcher, P. M., J. E. Longcore and M. J. Powell. 2014b. *Irineochytrium*, a new genus in *Chytridiales* having zoospores and aplanospores. *Mycologia* 106: 1188-1198.
- Letcher, P. M., M. J. Powell and W. J. Davis. 2018. Morphology, zoospore ultrastructure, and molecular position of taxa in the *Asterophlyctis* lineage (*Chytridiales*, *Chytridiomycota*). *Fungal Biol.* 122: 1109-1123.
- Picard, K., P. M. Letcher and M. J. Powell. 2009. *Rhizidium phycophilum*, a new species in the *Chytridiales*. *Mycologia* 101: 696-706.
- Powell, M. J. and W. J. Koch. 1977. Morphological variations in a new species of *Entophlyctis*. II. Influence of growth conditions on morphology. *Canad. J. Bot.* 55: 1686-1695.
- Powell, M. J., P. M. Letcher and J. E. Longcore. 2013. *Pseudorhizidium* is a new genus with distinct zoospore ultrastructure in the order *Chytridiales*. *Mycologia* 105: 496-507, doi:10.3852/12-269
- Powell, M. J., P. M. Letcher, J. E. Longcore and W. H. Blackwell. 2018. *Zopfochytrium* is a new genus in the *Chytridiales* with distinct zoospore ultrastructure. *Fungal Biol.* 122:1041-1049, doi.org/10.1016/j.funbio.2018.08.005
- Powell, M. J., P. M. Letcher, W. J. Davis, E. Lefèvre and M. Brooks. 2019. Taxonomic summary of *Rhizoclostratium* and description of four new *Rhizoclostratium* species (*Chytriomycetaceae*, *Chytridiales*). *Phytologia* 101(2): 139-163.
- Roane, M. K. and R. A. Paterson. 1974. Some aspects of morphology and development in the *Chytridiales*. *Mycologia* 66: 147-164.
- Seto, K. and Y. Degawa. 2018. *Pendulichytrium sphaericum* gen. et sp. nov. (*Chytridiales*, *Chytriomycetaceae*), a new chytrid parasitic on the diatom, *Aulacoseira granulata*. *Mycoscience* 59: 59-66.
- Seto, K., M. Kagami and Y. Degawa. 2017. Phylogenetic position of parasitic chytrids on diatoms: characterization of a novel clade in *Chytridiomycota*. *J. Eukaryot. Microbiol.* 64: 383-393.
- Sparrow, F. K. 1960. *Aquatic Phycomycetes*. 2nd rev. ed. Ann Arbor, Michigan: The University of Michigan Press. 1187 p.
- Vélez, C. G., P. M. Letcher, S. Schultz, M. J. Powell and P. F. Churchill. 2011. Molecular phylogenetic and zoospore ultrastructural analyses of *Chytridium olla* establish the limits of a monophyletic *Chytridiales*. *Mycologia* 103: 118-130, doi:10.3852/10-001
- Vélez, C. G., P. M. Letcher, S. Schultz, G. Mataloni, E. Lefèvre and M. J. Powell. 2013. Three new genera in *Chytridiales* from aquatic habitats in Argentina. *Mycologia* 105: 1251-1265, doi:10.3852/12-353
- Willoughby, L. G. 1961. Chitinophilic chytrids from lake muds. *Trans. Brit. Mycol. Soc.* 44: 586-592.

Table 1. Strains used for phylogenetic analysis				
Strain	GenBank Number	Location of Collection	Habitat	Substrate
		Ingroup		
ARG 12	JX905504	ARG, Buenos Aires Province, Partido de Escobar	aquatic	pollen
ARG 37	JX905505	ARG, Rio de la Plata River, Buenos Aires City	aquatic	pollen
ARG 39	JX905506	ARG, Corrientes Prov., Chañar Stream	aquatic	pollen
ARG 97	JX905513	ARG, Tierra del Fuego, Rancho Grande Peat Bog	peat bog	pollen
ARG 122	JX905520	ARG, Entre Rios Prov., Departamento de Villaguay, roadside pond	aquatic	pollen

BR 97	AY439074	Ramsayville Marsh, near Ottawa CANADA)	aquatic	moribund algae
JA 3	KC691314	USA, AL, Tuscaloosa, Lake Nicol	aquatic	pollen
JA 8	KU721090	USA, AL, Hale County, Vernal Pool, TNF ¹	soil	keratin
JEL 176	AY439064	USA, ME, Augusta, Viles Arboretum	aquatic	keratin
MP 5	AY988511	USA, MI, Pellston, Douglas Lake, Michigan Biological Station	aquatic	pollen
MP 41	JX905522	USA, AL, Tuscaloosa, West Side Stream, <i>Myriophyllum</i> roots	aquatic	pollen
MP 59	JX905525	USA, AL, Wheeler Wildlife Refuge, pond	aquatic	chitin
MP 60	*MK543212	USA, AL, Wheeler Wildlife Refuge, pond	aquatic	chitin
MP 61	*MK543213	USA, AL, Wheeler Wildlife Refuge, pond	aquatic	chitin
MP 66	KC691342	USA, AL, Northport, Road side ditch with <i>Spirogyra</i>	aquatic	pollen
MP 69	JX905526	USA, AL, Old Northport, Trestle, soil with <i>Vaucheria</i>	moist soil	pollen
MP 70	KC691345	USA, AL, Cottondale, Rainey Pond	aquatic	pollen
MP 72	*MK543214	USA, AL, Wagarville, Crawfish Pond	aquatic	chitin
MP 80	KC691348	USA, AL, Cottondale	moist soil	pollen
MP 89	KC691354	USA, AL, Tuscaloosa, Black Warrior River	aquatic	pollen
PL AUS 5	AY988512	AUS, NSW, Wingecarribe Shire, Fitzroy Falls	stream	pollen
PL AUS 14	AY422956	AUS, NSW, Ourimbah	soil	pollen
PL AUS 23	AY988514	TASMANIA, Sarah Island	soil	pollen
PL 148	*MK543218	USA, TX, Livingston, Alabama-Coushatta Indian Reservation	roadside ditch	pollen
PL 149	KF257912	USA, TX, Cold Spring, Sam Houston National Forest, Double Lake	aquatic	pollen
WB 216	KC691358	USA, AL, Cottondale, Rainey Pond	aquatic	moribund algae
WB 235A	DQ536493	USA, AL, Coker, Lake Lurleen, under alder tree	aquatic	dragonfly wing
WB 241	KC691366	USA, AL, Northport, North Wood Lake, Union Chapel Rd., <i>Myriophyllum</i> roots	mud	chitin
WB 266D	*MK543215	USA, NC, Lake Lure, Broad River, Bill Mt.	aquatic	chitin
WB 266E	*MK543216	USA, NC, Lake Lure, Broad River, Bill Mt.	aquatic	chitin
WB 266F	*MK543217	USA, NC, Lake Lure, Broad River, Bill Mt.	aquatic	chitin
WJD 131	JX905530	USA, AL, Cheaha	soil	cellulose
WJD 138	KC461388	USA, AL, Tuscaloosa, Black Warrior River	aquatic	pollen

WJD 183	KU721100	USA, AL, Hale County, Vernal Pool, TNF ¹	aquatic	dragonfly wing
JEL 794	*MK558057	USA, ME, Mud Pond, Hancock County	aquatic	chitin
		Outgroup		
JEL 222	DQ485551	<i>Rhizophydium globosum</i> USA, ME, Orono	soil	pollen
¹ Oakmulgee District of the Talladega National Forest (TNF) *Newly generated sequences				

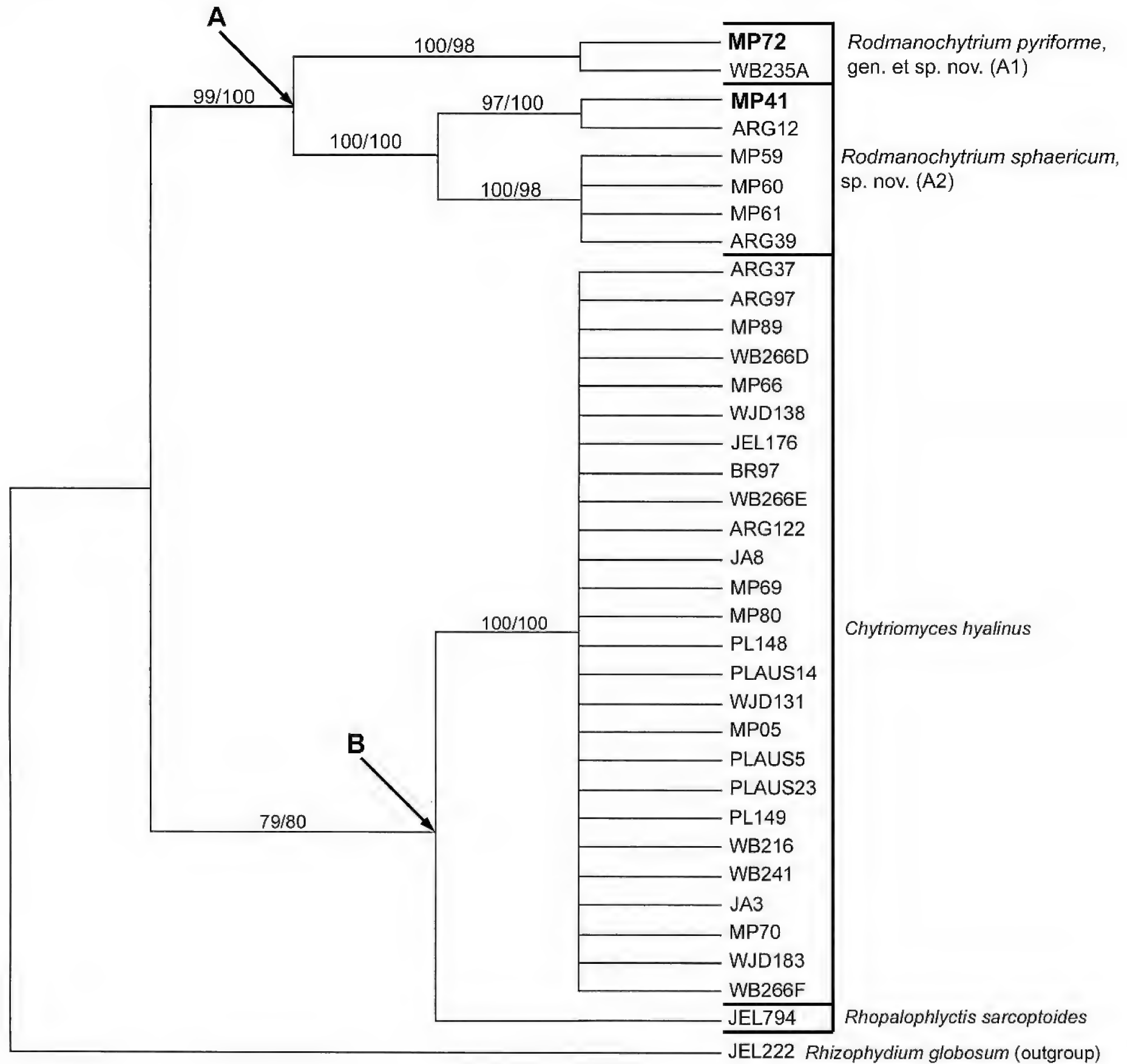


Figure 1. Molecular phylogenetic assessment. Cladogram inferred from strict consensus, maximum parsimony analysis of 35 strains in *Chytriomycetaceae* using 28S rDNA sequences. Numbers at nodes are bootstrap support values (maximum likelihood/maximum parsimony). Lineage A includes eight unidentified chitinophilic strains in two sub-clades (A1, A2), which represent *Rodmanochytrium pyriforme* gen. et sp. nov. (A1) and *R. sphaericum* sp. nov. (A2). Lineage A is sister of Lineage B. Lineage B includes representatives of two other chitinophilic species, *Rhopalophlyctis sarcoptoides* and the morpho-species *Chytriomycetes hyalinus*. Strain JEL 222 *Rhizophydium globosum* is the outgroup.

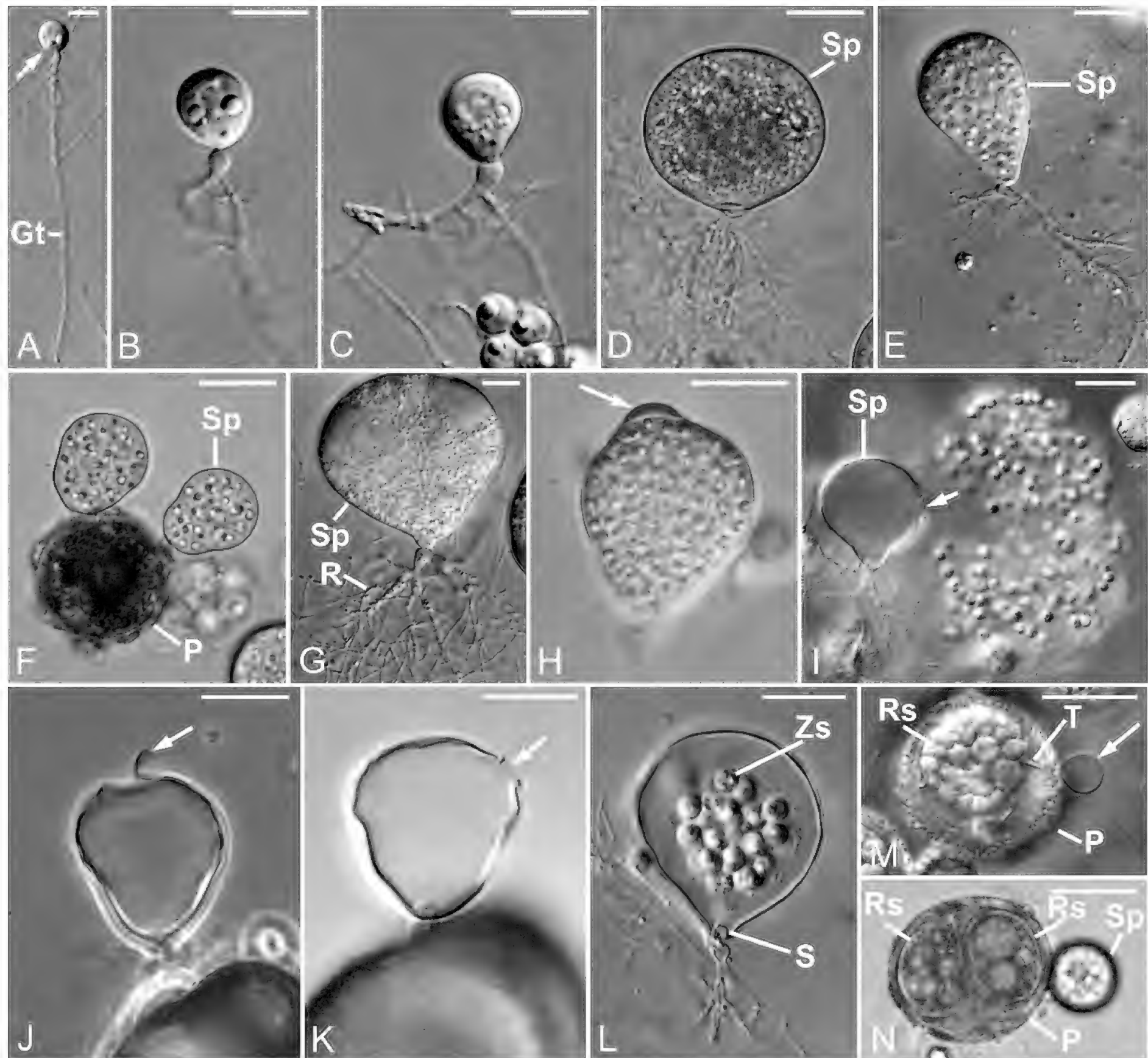


Figure 2. Light microscopy of thallus morphology of *R. pyriforme* sp. nov., strain MP 72. (A) Encysted zoospore (arrow) with long germ tube. (B) Germling with developing rhizoid; sub-sporangial portion of rhizoid spherical, dichotomously branching near enlarging encysted zoospore. (C) Developing thallus; incipient sporangium pyriform; sub-sporangial portion of rhizoidal axis broadly tubular; rhizoids branch dichotomously. (D) Oval sporangium with apical portion broadest and tapering toward the base. Rhizoids finely branched. (E) Clavate sporangium tapering toward base and containing cleaved zoospores. (F) Pollen grain with two pyriform sporangia attached. (G) Pyriform sporangium with narrow base and finely branched rhizoids. (H) Gelatinous plug formed below the forming operculum (arrow). (I) Vesicular zoospore discharge; empty sporangium is pyriform with lateral discharge pore (arrow). (J) Empty pyriform sporangium on pollen with operculum still attached to side of discharge pore (arrow). (K) Empty pyriform sporangium on pollen grain; sub-apical discharge pore with recurved edge (arrow). (L) Partially empty pyriform sporangium with dome-shaped septum. (M) Spherical resting spore in pollen; empty zoospore cyst at surface of pollen grain (arrow) with tube connected to resting spore. (N) Two oval resting spores inside of a pollen grain; developing sporangium attached to the surface of the pollen grain. Scale bar = 5 μ m (A), 10 μ m (B, C, G), 20 μ m (D, E, F, H-N). Abbreviations: Gt, germ tube; P, pollen; R, rhizoid; Rs, resting spore; S, septum; Sp, sporangium; T, tube; Zs, zoospore.

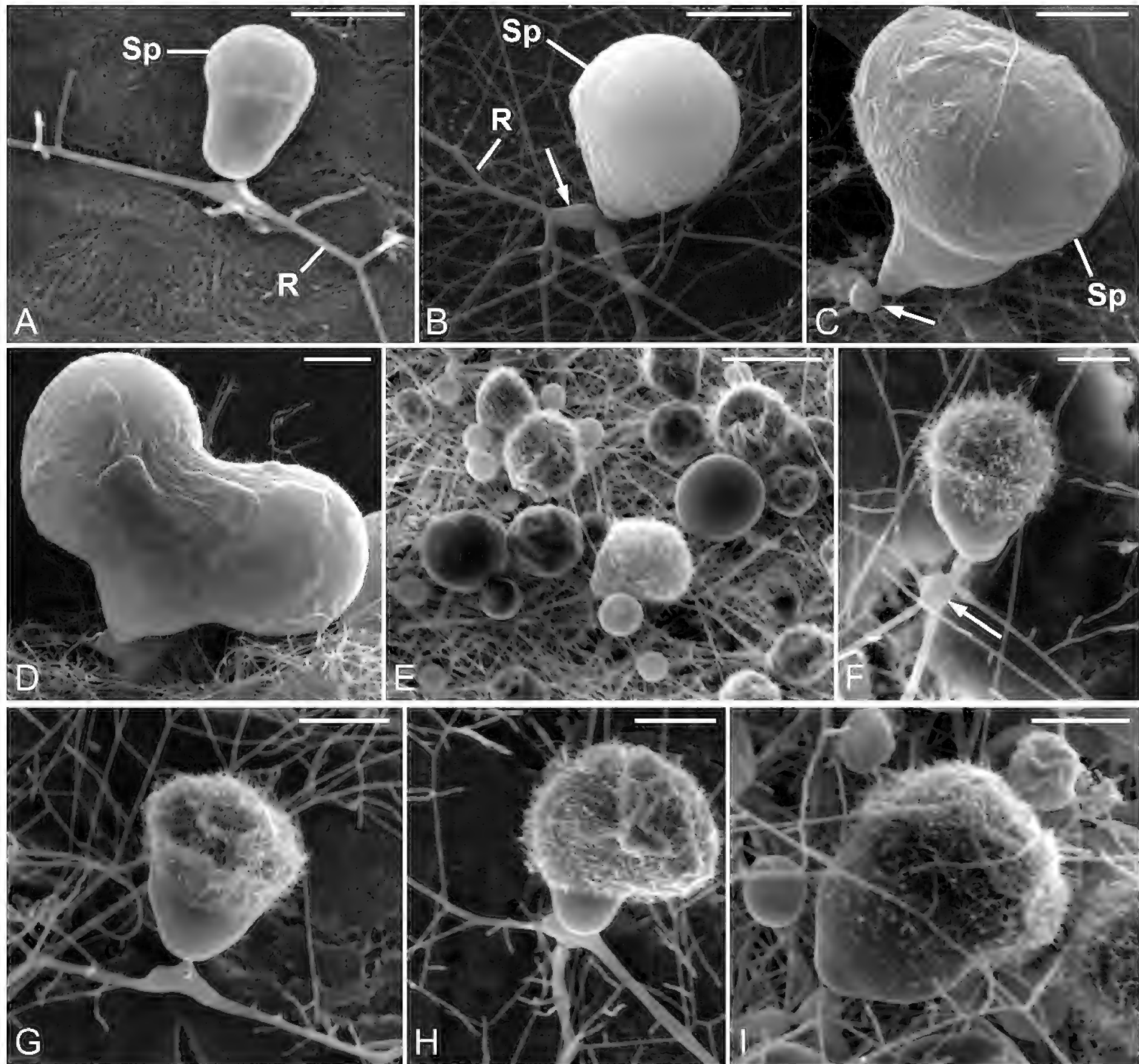


Figure 3. Scanning microscopy of thallus morphology of *R. pyriforme* sp. nov., strain MP 72; chitin substrate. (A, B) Developing pyriform sporangia, surfaces smooth. (C) Pyriform sporangium with rugose upper surface and spherical sub-sporangial rhizoidal connection (arrow). (D) Lobed sporangium with rugose surface. (E) Sporangia with smooth and hirsute surfaces. (F) Developing thallus; upper surface hirsute; rhizoid arises on sporangium as a short tube from a single point and with a small swelling formed (arrow). (G, H, I) Developing hirsute thalli; upper portion of sporangia covered with fine hair-like structures. Rhizoids branch near sporangium. Scale bar = 5 μm (A, F-I), 10 μm (B, C, D), 30 μm (E). Abbreviations: R, rhizoid; Sp, sporangium.

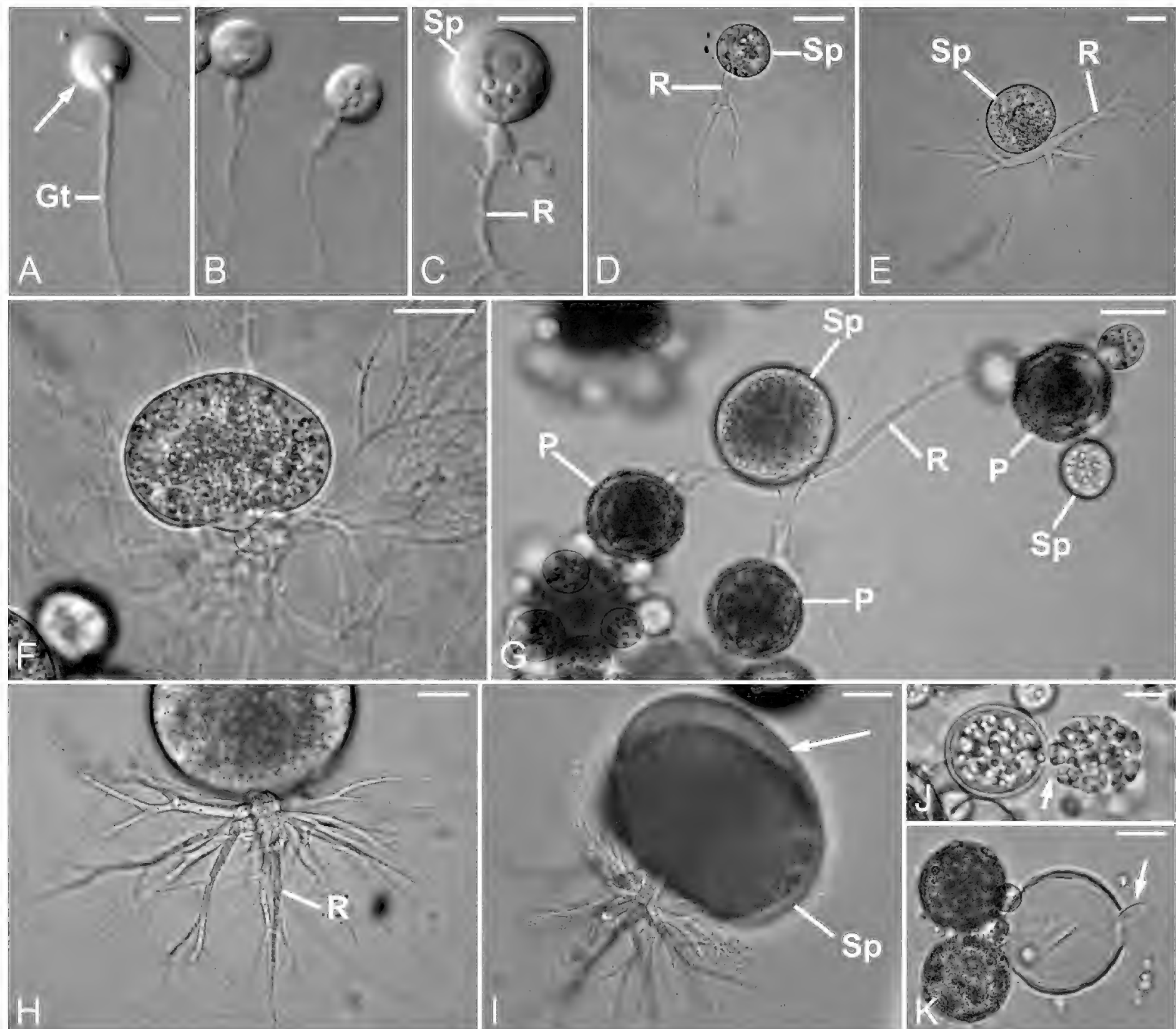


Figure 4. Light microscopy of thallus morphology of *R. sphaericum* sp. nov., strain MP 41. (A) Encysted zoospore (arrow) with elongate germ tube. (B) Two germlings; rhizoidal axis swollen at base of incipient sporangium. (C) Developing thallus; incipient sporangium spherical; rhizoidal axis swollen near sporangium and dichotomously branched. (D) Developing thallus; trunk-like main rhizoidal axis extends with fine branches. (E) Developing thallus; rhizoidal axis stout near sporangium and branching dichotomously. (F) Oval sporangium; basal portion cup-shaped; sub-sporangial rhizoidal axis connection bulbous. (G) Thallus development on pollen illustrating range in sporangial diameters; small epibiotic sporangia; larger interbiotic thallus; sporangia spherical. (H) Rhizoidal system arises from short sub-sporangial tube as stout branches; branching dichotomously into fine branches. (I) Oval sporangium with bushy rhizoidal system. Cytoplasm in sporangium forms zones (arrow). (J) Vesicular zoospore discharge (arrow) from spherical sporangium. (K) Empty spherical sporangium with operculum attached to rim of discharge pore (arrow). Scale bar = 5 μm (A), 10 μm (B, C, J, K), 20 μm (D, E-I). Abbreviations: Gt, germ tube; P, pollen; R, rhizoid; Sp, sporangium.

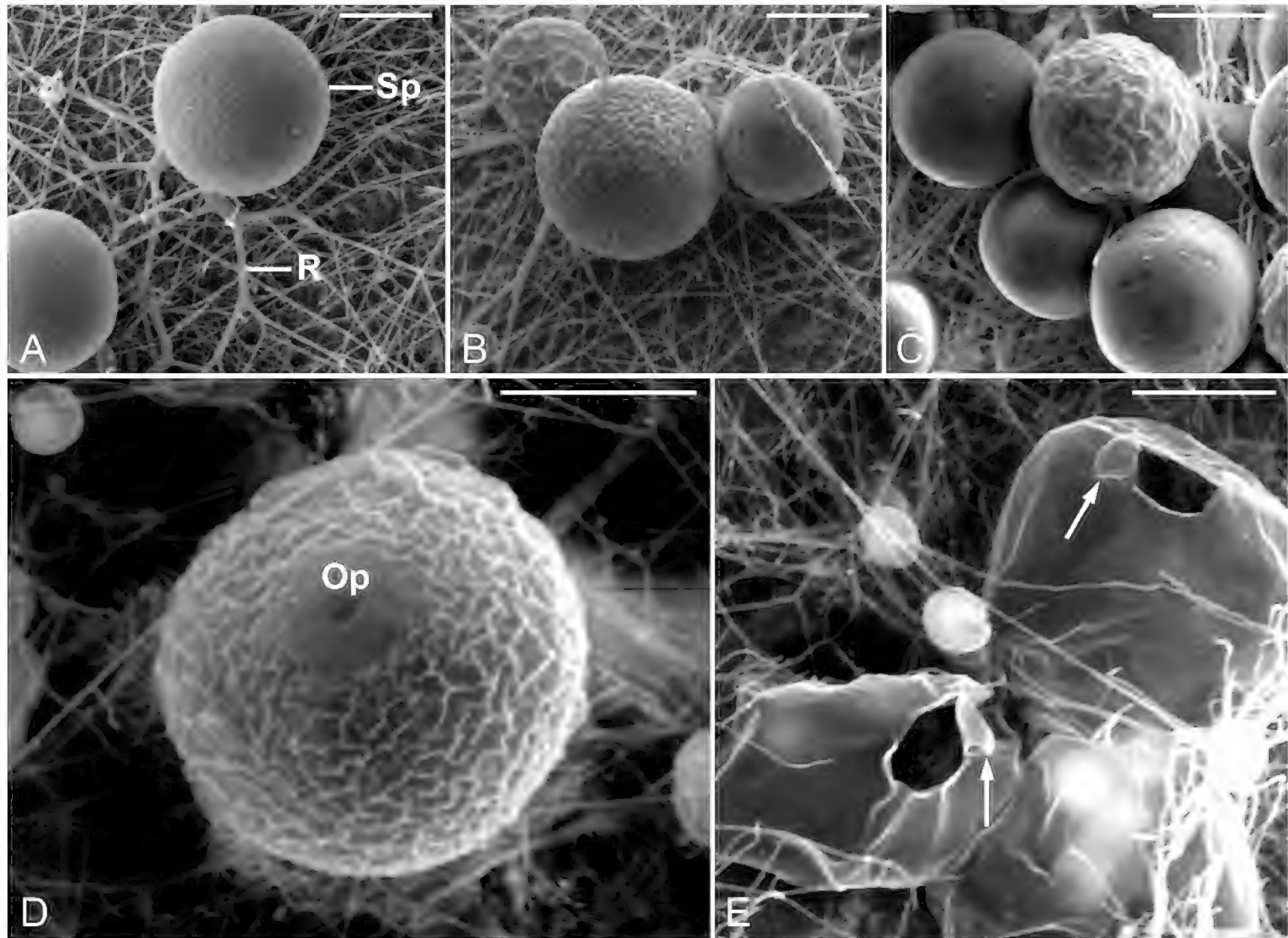


Figure 5. Scanning electron microscopy of thallus morphology of *R. sphaericum* sp. nov., strain MP 41; chitin substrate. (A) Spherical sporangium with finely-granular surface; rhizoidal axis near sporangium stout and branching dichotomously. (B) Sporangia with finely-granular, reticulate and smooth surfaces. (C) Sporangia with reticulate and smooth surfaces. (D) Sporangium with reticulate surface; area over the operculum is smooth. (E) Empty sporangia with smooth surfaces; operculum still attached to the side of the discharge pore (arrow). Scale bar = 10 μ m (A-E). Abbreviations: Op, operculum; R, rhizoid; Sp, sporangium.